



저작자표시-비영리-변경금지 2.0 대한민국

이용자는 아래의 조건을 따르는 경우에 한하여 자유롭게

- 이 저작물을 복제, 배포, 전송, 전시, 공연 및 방송할 수 있습니다.

다음과 같은 조건을 따라야 합니다:



저작자표시. 귀하는 원저작자를 표시하여야 합니다.



비영리. 귀하는 이 저작물을 영리 목적으로 이용할 수 없습니다.



변경금지. 귀하는 이 저작물을 개작, 변형 또는 가공할 수 없습니다.

- 귀하는, 이 저작물의 재이용이나 배포의 경우, 이 저작물에 적용된 이용허락조건을 명확하게 나타내어야 합니다.
- 저작권자로부터 별도의 허가를 받으면 이러한 조건들은 적용되지 않습니다.

저작권법에 따른 이용자의 권리는 위의 내용에 의하여 영향을 받지 않습니다.

이것은 [이용허락규약\(Legal Code\)](#)을 이해하기 쉽게 요약한 것입니다.

[Disclaimer](#)

의학박사 학위논문

딥러닝을 이용한  
한국형 소아 골연령 표준 영상 구축 및  
골연령 자동 판정 시스템 개발

A Deep Learning-Based Pediatric Bone Age Assessment  
in Korean Pediatric Population: Comparison with  
Greulich and Pyle Based System and Development of  
Korean Standard Atlas

울산대학교 대학원

의학과

김평화

A Deep Learning-Based Pediatric Bone Age Assessment  
in Korean Pediatric Population: Comparison with  
Greulich and Pyle Based System and Development of  
Korean Standard Atlas


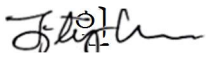

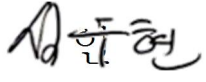
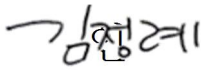
지 도 교 수 이 진 성

이 논문을 의학박사 학위 논문으로 제출함

2022년 06월

울 산 대 학 교 대 학 원  
의 학 과  
김 평 화

김평화의 의학박사 학위 논문을 인준함

심사위원	이 상 훈	
심사위원	이 진 성	
심사위원	윤 희 망	
심사위원	심 우 현	
심사위원	김 정 례	

울 산 대 학 교 대 학 원

2022년 06월

## ABSTRACT

**Objective:** To develop and validate a deep learning-based bone age prediction model using hand radiographs in healthy Korean children and adolescents by making comparison with Greulich-Pyle based deep learning based model (GP based model), and to develop a Korean standard Atlas.

**Materials and Methods:** A convolutional neural network (Korean standard model) was trained to predict chronologic age using 21,036 hand radiographs of Korean children and adolescents with a normal bone development from Asan Medical Center obtained between 1998 and 2019. External validation was conducted using two separate datasets from Pusan National University Yangsan Hospital (Institution 1; n=304) and Dankook University Hospital (Institution 2; n=314). Mean absolute error (MAE), root mean square error (RMSE), proportions of bone age predictions within 6, 12, 18, and 24 months of chronologic age were compared with GP-based model. Bland-Altman plot analysis was additionally performed. Subgroup analysis restricted to age 2–16 for male, and 2–14 for female was conducted.

**Results:** Compared to GP, Korean standard model showed a lower RMSE (10.2 vs. 12.4 months;  $P<.001$ ), MAE (7.6 vs. 9.7 months;  $P<.001$ ), and higher proportions of bone age predictions within 12 ( $P<.04$ ) and 18 months ( $P<.007$ ) in Institution 1. MAE of Korean standard model was lower (10.9 vs. 9.6 months;  $P<.008$ ) in Institution 2. In the subgroup analysis, Korean standard model showed lower RMSE and MAE (all  $P<.001$ ) and higher proportions of bone age predictions within 6, 12, and 18 months (all  $P<.05$ ). Furthermore, systemic trend differences in GP based model were reduced in Korean standard model (Institution 1,  $P<.001$  to .27; Institution 2,  $P<.001$  to .048). Korean standard atlas was developed and finalized by a consensus meeting.

**Conclusion:** A deep learning based Korean standard bone age assessment model a better performance than GP based bone age assessment model in healthy Korean children and adolescents, by reflecting a characteristic skeletal maturation in contemporary Korean children and adolescents. A Korean standard atlas of bone age based on a Korean standard model was newly introduced.

## Contents

ABSTRACT .....	i
INTRODUCTION .....	1
MATERIALS AND METHODS .....	2
Study Design and Dataset .....	2
Model Development: Preprocessing .....	3
Model Development: Convolutional Neural Networks .....	3
External Validation .....	4
Korean Standard Atlas Development .....	4
Statistical Analysis .....	5
RESULTS .....	7
Dataset Characteristics .....	7
Internal Validation .....	9
External Validation .....	9
Subgroup Analysis .....	13
Korean Standard Atlas Development .....	16
DISCUSSION .....	17
REFERENCE LIST .....	20
국문요약 .....	23
APPENDIX .....	24
Korean Standard Atlas: Male .....	24
Korean Standard Atlas: Female .....	53

## INTRODUCTION

Bone age, generally evaluated using hand and wrist radiographs, is a representative index reflecting skeletal maturation of children and adolescents. Growth disorder can be considered when a considerable discrepancy between the chronologic age and bone age observed (e.g., discrepancy > 2 standard deviation [SD]) (1, 2). In addition, bone age is useful for surgical decisions in orthopedics (3) and forensic issues (4). Among the several methods for bone age determination, the atlas-based Greulich and Pyle (GP) method is one of the most widely used method (5). However, unsolved issues regarding the conventional GP method have been addressed – there is no standardized protocol which bone should be more weighted for the assessment of bone age, leading an unignorable inter, intraobserver, and inter-institutional variability (6-8). For this reason, an automated GP-based bone age prediction system has been introduced and demonstrated high accuracy, reproducibility, and time-efficiency (9-11).

However, it is still questionable whether this method could be applicable to the current Korean pediatric population, as GP method was derived from white pediatric population of upper socioeconomic level almost a century ago (5). Indeed, one meta-analysis demonstrated significant differences between the bone age and chronologic age in Asian boys (12). Furthermore, Zhang et al. showed the advanced bone age based on GP method in Asian boys (11–15 years) and girls (10–13 years) compared to Caucasian (13), and Ontell et al. also reported the delayed bone age in preadolescent period and advanced bone age in adolescent period for Asian boys (14). A standard bone age chart based on Tanner-Whitehouse 2 (TW2)-20 score by using 3407 radiographs of Korean children was introduced in 1996 (15). However, the relatively small sample size and considerable time required for the assessment based on TW2 method (16) limited a wide application to real practice.

In this context, a deep learning-based bone age prediction model focusing on Korean pediatric population has a potential value in that it could offer a simple and reproducible bone age assessment optimized for Korean pediatric population reflecting those ethnic and environmental factors. In addition, it may be possible to develop a standard Korean atlas comprising reference images of a specific age, potentially serve as a guide for the accurate growth evaluation in Korean children and adolescents. Therefore, we aimed to develop a deep

learning based bone age prediction model using hand and wrist radiographs obtained in healthy Korean children and adolescents with a ground truth as chronologic age, to validate its feasibility by comparison with a GP-based deep learning bone age assessment system, and then to develop a Korean standard Atlas based on a new deep learning algorithm.

## **MATERIALS AND METHODS**

This retrospective study was conducted in accordance with Checklist for Artificial Intelligence in Medical Imaging (17). Approval from the institutional review board was obtained by each participating institution. Informed patient consent was waived by the institutional review board due to the retrospective nature of the study.

### *Study Design and Dataset*

Since our primary goal was to develop a chronologic-age-prediction model based on a healthy Korean pediatric population (Korean standard model), we collected left hand and wrist radiographs of Korean children and adolescents who expected to show a probable normal bone development without any genetic, endocrinologic, or other chronic disease. Therefore, a systematic, computerized search of the database of our institution (Asan Medical Center; reference institution) was initially performed in a retrospective and consecutive manner to identify all left hand and wrist radiographs of eligible pediatric patients (age <19 years) obtained between 1998 and 2019. Then, we excluded radiographs of the patients if any of the following exclusion criteria met: (a) confirmed precocious puberty; (b) confirmed delayed puberty (absent secondary sexual character in male  $\geq 15$  or female  $\geq 14$  years); (c) abnormal growth rate in peripubertal period compared to other Korean pediatric population of same age; (d) abnormally short stature compared to other Korean pediatric population of same age (i.e., height less than 3rd percentile for age and gender according to the Korean population-based reference) (18); (e) confirmed congenital anomalies; (f) underlying chronic disease potentially affecting growth; (g) use of medications affecting bone development, i.e., growth hormone therapy or vitamin D; (h) evident tumors noted on the radiographs; (i) fractures with/without dislocations noted on the radiographs; (j) amputation or excision state; (k) radiographs with



poor image quality or wrong patient positioning. Images were initially screened by one researcher (B.P., 2 years of clinical experience as a radiology technicians; P.H.K., 2 years of experience in pediatric radiology), and double-checked by a pediatric radiologist for the randomly selected, initially screened radiographs (P.H.K.; 2 years of experience in pediatric radiology). Then, for the radiographs with any of a potential to be excluded identified, two radiologists determined those to be satisfactory for bone age assessment (H.M.Y. and P.H.K.; 9 and 2 years of experience in pediatric radiology, respectively).

#### *Model Development: Preprocessing*

For training our deep learning model, the input of the model passes several preprocessing modules to achieve consistency in data quality and reduce data complexity. First, the images were resized into a uniform size of 512 x 512 pixels. Then, the background removal module was performed on the downsampled image. Finally, a series of transformations (translation and rotation) was performed to make the scale and position of the hand of all x-ray data constant.

#### *Model Development: Convolutional Neural Networks*

A deep convolutional neural networks model called ResNet-50 (19) was used for estimating the chronological age by 1-month interval. After each convolutional layer, a “ReLU” activation function was employed for non-linearity, and batch normalization was performed to avoid overfitting. Finally, the flattened feature vectors from the global average pooling layer were fed into a last fully connected layer which has 256 nodes. Each node of the last fully connected layer corresponds to the patient's chronological age converted by 1-month interval. To accelerate model convergence and get better estimation performance, parameters of the model were pretrained on ImageNet (20) except for the last fully connected layer whose biases were set to zeros, and all the weights were randomly initialized, ranging from -0.5 to 0.5. We trained our chronological age prediction model by minimizing an objective function called DLDLv2 (21): data augmentations with random rotation, scale, horizontal flipping and Adam optimizer. Initial learning rate was 1e-3 and dropped to 1e-5. Training epochs were 300. Models were trained using the PyTorch 1.7 (<https://pytorch.org>) in Python 3.6. Performance

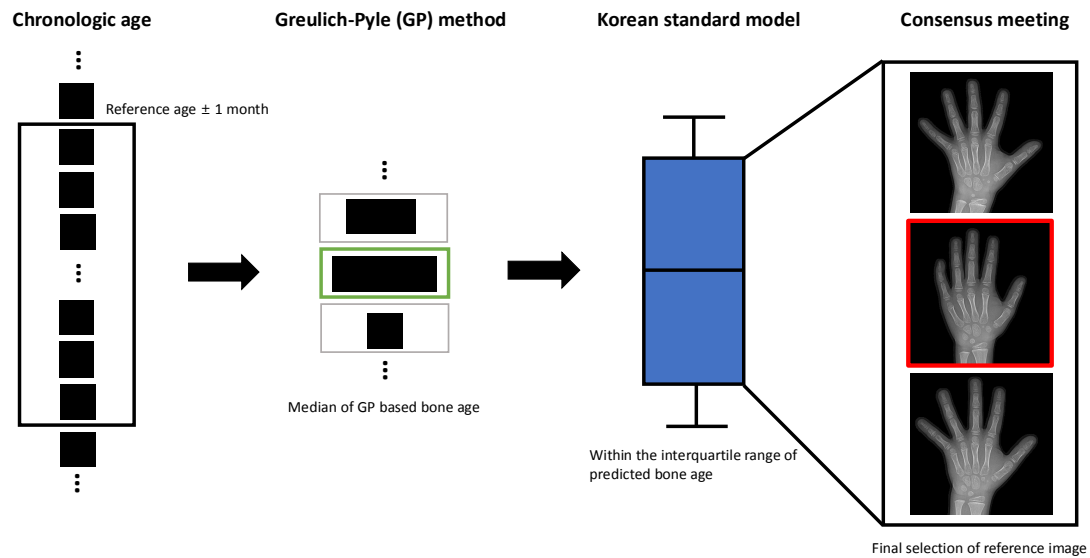
of the developed Korean standard model was internally validated using four-fold cross-validation.

#### *External Validation*

For the external validation, we obtained two separate datasets from Pusan National University Yangsan Hospital (Institution 1) and Dankook University Hospital (Institution 2), comprising left hand and wrist radiographs of Korean children and adolescents obtained in clinical setting of trauma. Radiographs were included only if two radiologists determined those to be satisfactory for bone age assessment (H.M.Y. and P.H.K.; 9 and 2 years of experience in pediatric radiology, respectively).

#### *Korean Standard Atlas Development*

We aimed to develop Korean Standard atlas comprising representative left wrist and hand radiographs from 0 to 24 months at 6-month intervals, and from 24 months to 19 years for boys and 18 years for girls at 1-year intervals. In order to select the most representative images in a specific age group, subjects with a difference in chronologic age less than 1 month from the reference age (ex. 23- to 25-month-old children for the 24-month standard) were initially selected. Then, the results by a commercialized, GP based automated bone age prediction model (GP based model) were extracted. In this, the predicted bone age by the GP based model was regarded as an indicator reflecting a skeletal maturation, and used for the arrangement of radiographs in order according to a skeletal maturation. We selected the radiographs in which the predicted bone age by GP based model was median of the initially selected subjects under the assumption that degree of their bone maturity is representative of each specific age group. Among them, we additionally selected the radiographs in which the predicted bone age by Korean standard model did not deviate from the IQR of each specific age group. Finally, the reference image was selected among the images of those selected subjects by a consensus meeting consisting of four pediatric radiologists (J.S.L., H.M.Y., J.H., and P.H.K., 30, 9, 5, and 2 years of experience in pediatric radiology, respectively).



**Figure 1.** Illustration for the selection of reference images in Korean Standard atlas.

### *Statistical Analysis*

The developed Korean standard model was externally validated in two separated datasets from Institution 1 and Institution 2. In our study, the ground truth reference standard was chronologic age. For the comparison, a commercially available GP based model (VUNO Med-BoneAge, version 1.1.0, VUNO) was applied to those datasets. The performance of each system was first estimated by Pearson correlation coefficients with a scatterplot. Of note, for the statistical analysis, the predicted bone age of the GP based model was calculated by the summation of all BAs multiplied by each predicted probabilities (i.e., VUNO score). Mean absolute error (MAE) and root mean square error (RMSE) were also calculated. In addition, MAE and RMSE were compared between Korean standard model and GP based model by using generalized estimating equation to account for patient clustering effects. The proportion of bone age predictions within 6, 12, 18, and 24 months of chronologic age were calculated and compared between Korean standard model and GP based model using a chi-square test. In addition, Bland-Altman plot analysis was performed between both chronologic age and the predicted age from Korean standard model, and chronologic age and the predicted age from GP based model to identify any systemic difference between the measurements. The presence of systemic trend differences between the chronologic age and the predicted age was assessed by using an univariable linear regression analysis based on the Bland-Altman plot, with the

independent variable as mean value of the chronologic age and predicted bone age, and with the dependent variable as difference between the chronologic age and predicted bone age.

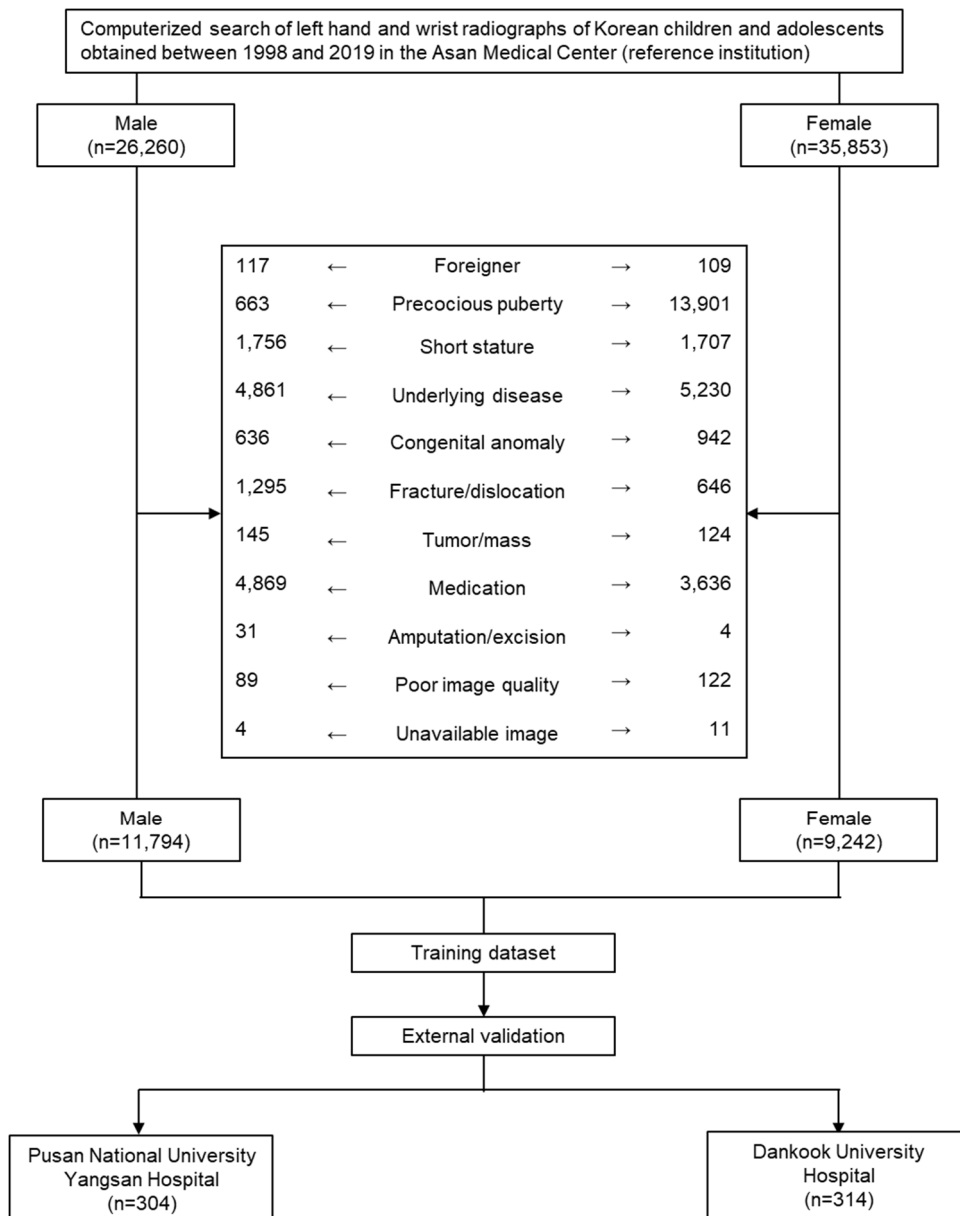
Given that GP based model has shown suboptimal predictive performance in the age < 2 years (22) and GP has upper limit of age grouping, we performed a subgroup analysis restricted to age 2–16 for male, and 2–14 for female. Pearson correlation coefficient analysis, MAE, RMSE, and Bland-altman plot analysis were performed in both Korean standard model and GP based model as a same manner.

Generalized estimating equation was performed using IBM SPSS Statistics for Windows (version 23.0; IBM Corp, Armonk, NY), and the other statistical analyses were performed using R software (version 3.6.3.; R Foundation for Statistical Computing, Vienna, Austria). A value of  $p < 0.05$  was taken to indicate statistical significance.

## RESULTS

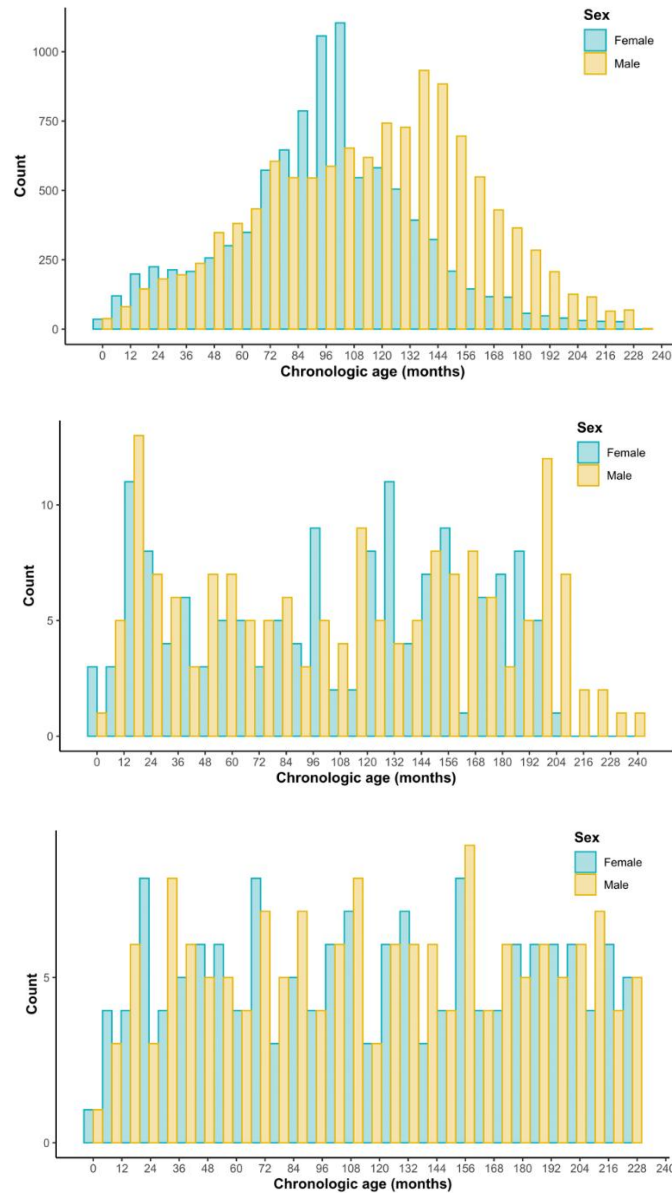
### *Dataset Characteristics*

Among the 62113 radiographs identified by a computerized search, a total of 21036 radiographs from the reference institution (median age [interquartile range; IQR], 9 [7–12] years; male:female, 11794:9242) were used for the model development (Figure 2).



**Figure 2.** Flow diagram for patient selection and dataset organization.

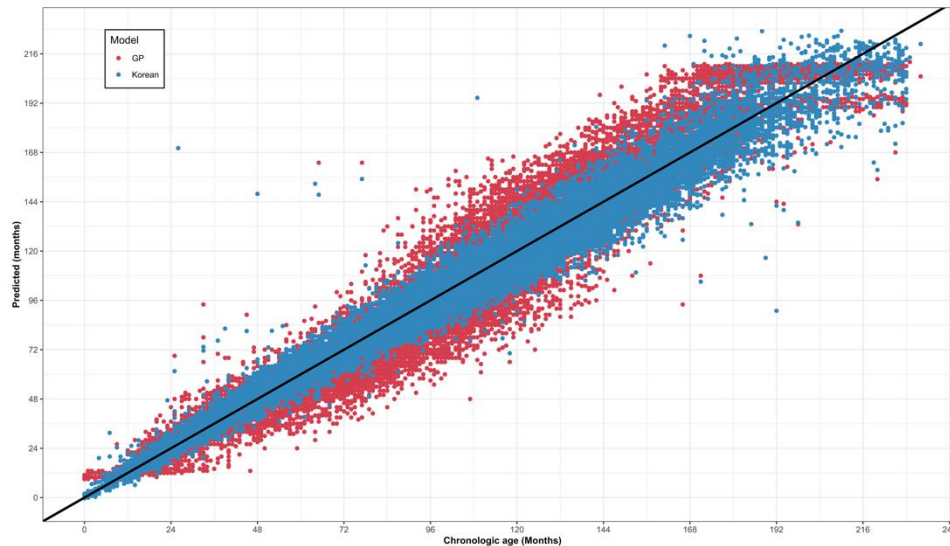
For the external validation, 304 radiographs from Institution 1 (median age [interquartile range], 9 [4–13] years; male:female, 163:141) and 314 radiographs from Institution 2 (median age [IQR], 9 [5–14] years; male:female, 160:154) were used. The distributions of ages for those datasets are shown in Figure 3.



**Figure 3.** A histogram showing chronologic age distribution of the datasets from the (A) reference institution, (B) institution 1, and (C) institution 2.

### *Internal Validation*

The bivariate scatterplot showing the association with chronologic age and the predicted bone age by GP based model and Korean standard model is presented in Figure 4.



**Figure 4.** A bivariate scatterplot showing association between chronologic age and predicted bone age by Greulich-Pyle based (red dots) and Korean standard model (blue dots). Perfect concordance is represented by a 45-degree line (black line).

The RMSE and MAE were 8.4 and 6.1 years for Korean standard model, and 12.6 and 10.0 years for GP based model. The proportions of the subjects with absolute difference  $\leq 6, 12, 18,$  and 24 months were significantly higher in Korean standard model ( $\leq 6$  months, 36.3% [7639 of 21036] vs. 60.7% [12770 of 21036];  $\leq 12$  months, 62.0% [13048 of 21036] vs. 87.5% [18408 of 21036];  $\leq 18$  months, 79.8% [16781 of 21036] vs. 96.3% [20266 of 21036];  $\leq 24$  months, 90.7% [19084 of 21036] vs. 98.8% [20774 of 21036]; all  $P < .001$ ).

### *External Validation*

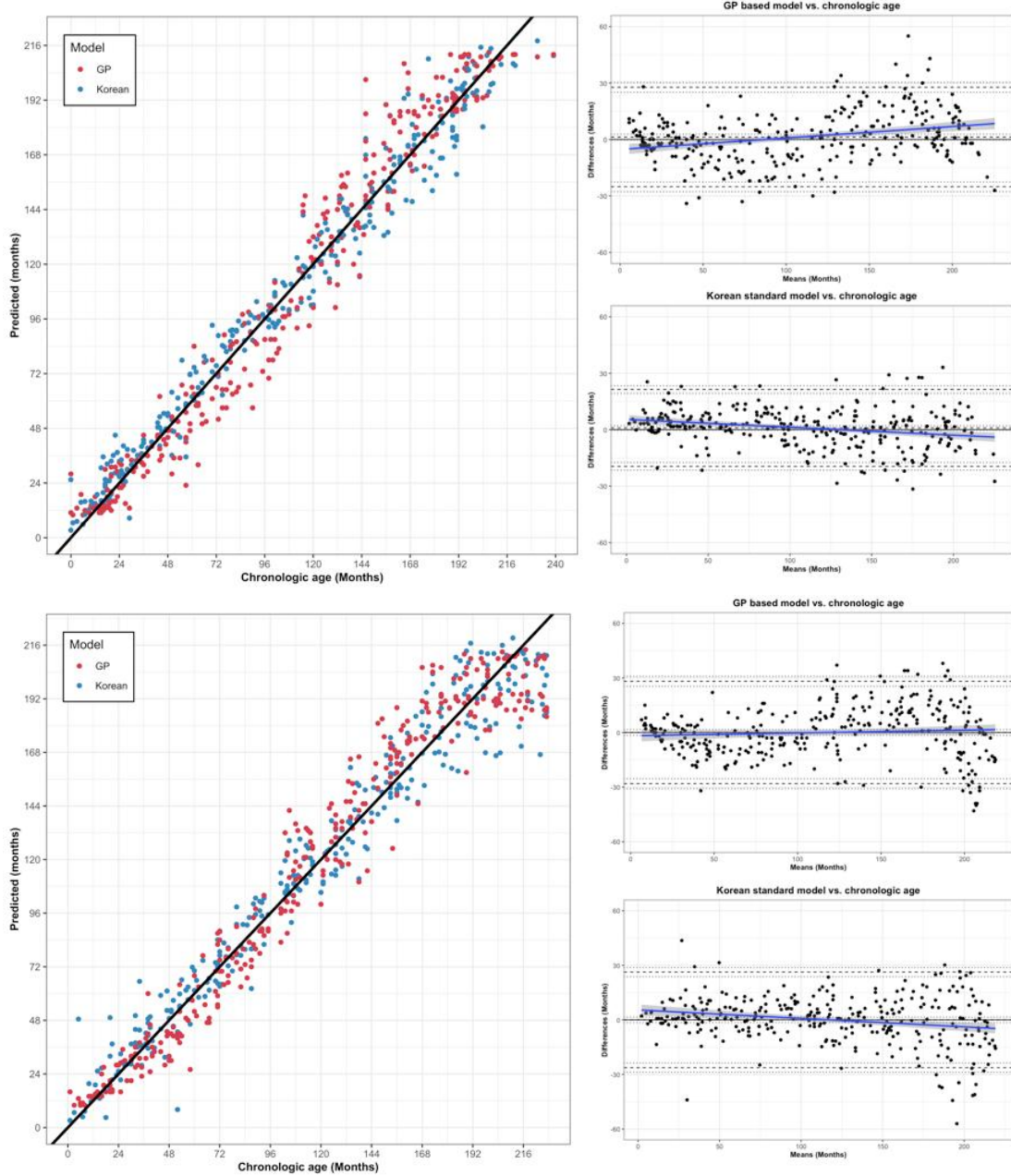
Prediction values from concordance analysis between the chronological age and predicted bone age by GP based model and Korean standard model are summarized in Table 1 and Figure 5.

**Table 1.** Concordance between chronological age and predicted bone age by Greulich-Pyle based model and Korean standard model.

Parameters	Institution 1			Institution 2		
	GP	Korean	P-value	GP	Korean	P-value
RMSE (months)	12.4	10.2	<.001	14.1	13.3	.20
MAE (months)	9.7	7.6	<.001	10.9	9.6	.008
% of subjects with absolute difference						
≤ 6 months	43.4 (131/302)	49.0 (148/302)	.19	36.1 (113/313)	43.5 (136/313)	.07
≤ 12 months	69.5 (210/302)	77.2 (233/302)	.04	65.8 (206/313)	70.9 (222/313)	.20
≤ 18 months	83.4 (252/302)	91.1 (275/302)	.007	81.5 (255/313)	85.3 (267/313)	.24
≤ 24 months	93.0 (281/302)	96.4 (291/302)	.10	90.7 (284/313)	91.1 (285/313)	>.99

RMSE = root mean square error; MAE = mean absolute error; GP = Greulich-Pyle.





**Figure 5.** Bivariate scatterplots showing association between chronologic age and predicted bone age by Greulich-Pyle (GP) based (red dots) and Korean standard model (blue dots) and Bland-Altman plots showing a difference between the chronologic age and the predicted bone age in (A) Institution 1 and (B) Institution 2 datasets. In a bivariate scatter plot, perfect concordance is represented by a 45-degree line (black line). In a Bland-Altman plot, the top and bottom dashed lines denote 1.96 standard deviations above and below the mean difference. The dotted line represents 95% confidence intervals for these three values. A black line at 0 is the reference representing no bias (mean or slope) exists. The blue line represents the estimated

bias from 0 with respect to age with 95% confidence intervals (gray shaded area). Note that systemic trend differences of GP model are observed in Institution 1 (slope, 0.061;  $P < .001$ ), and those of Korean model are observed both in Institution 1 (slope, -0.042;  $P < .001$ ) and Institution 2 (slope, -0.046;  $P < .001$ ).

In Institution 1, both RMSE and MAE were significantly lower in Korean standard model than GP based model (RMSE, 10.2 vs. 12.4 months [ $P < .001$ ]; MAE, 7.6 vs. 9.7 months [ $P < .001$ ]). In addition, the proportions of the subjects with absolute difference  $\leq 12$  months (69.5% vs. 77.2%;  $P = .04$ ) and  $\leq 18$  months (83.4% vs. 91.1%;  $P = .007$ ) were also higher in Korean standard model. In Institution 2, MAE was significantly lower in Korean standard model (10.9 vs. 9.6 months;  $P = .008$ ). We did not find any statistical difference of RMSE and the proportion of the subjects with the absolute difference  $\leq 6, 12, 18,$  and 24 months in Institution 2.

The Bland-Altman results are summarized in Table 2 and Figure 5. Both GP based model and Korean standard model predicted higher bone age than chronological age. Korean standard model showed a systematic trend to underestimate the age as the chronologic age increased (Institution 1; slope, -0.042;  $P < .001$ ; Institution 2, slope, -0.046;  $P < .001$ ). GP based model showed a systematic trend to overestimate the age as the chronologic age increased in Institution 1 (slope, 0.061;  $P < .001$ ), but we found no systematic trend in Institution 2.

**Table 2.** Bland-Altman Results for relationships between chronological age and predicted bone age (Greulich-Pyle based model vs. Korean standard model).

Parameters	Institution 1		Institution 2	
	GP	Korean	GP	Korean
Slope	0.061	-0.042	0.015	-0.046
Intercept	-5.3	5.5	-1.8	5.5
Bias	1.311	0.952	0.035	0.020
Standard deviation	13.486	10.413	14.350	13.380
95% limits of agreement	-25.1–	-19.5–	-28.1–	-26.2–
	27.7	21.4	28.2	26.2
P-value <sup>a</sup>	<.001	<.001	0.22	<.001

GP = Greulich-Pyle.

<sup>a</sup>P-value was calculated using the univariable linear regression analysis based on the Bland-Altman plot, with the independent variable as mean value of the chronological age and predicted bone age and the dependent variable as difference between the chronological age and predicted bone age.

#### *Subgroup Analysis*

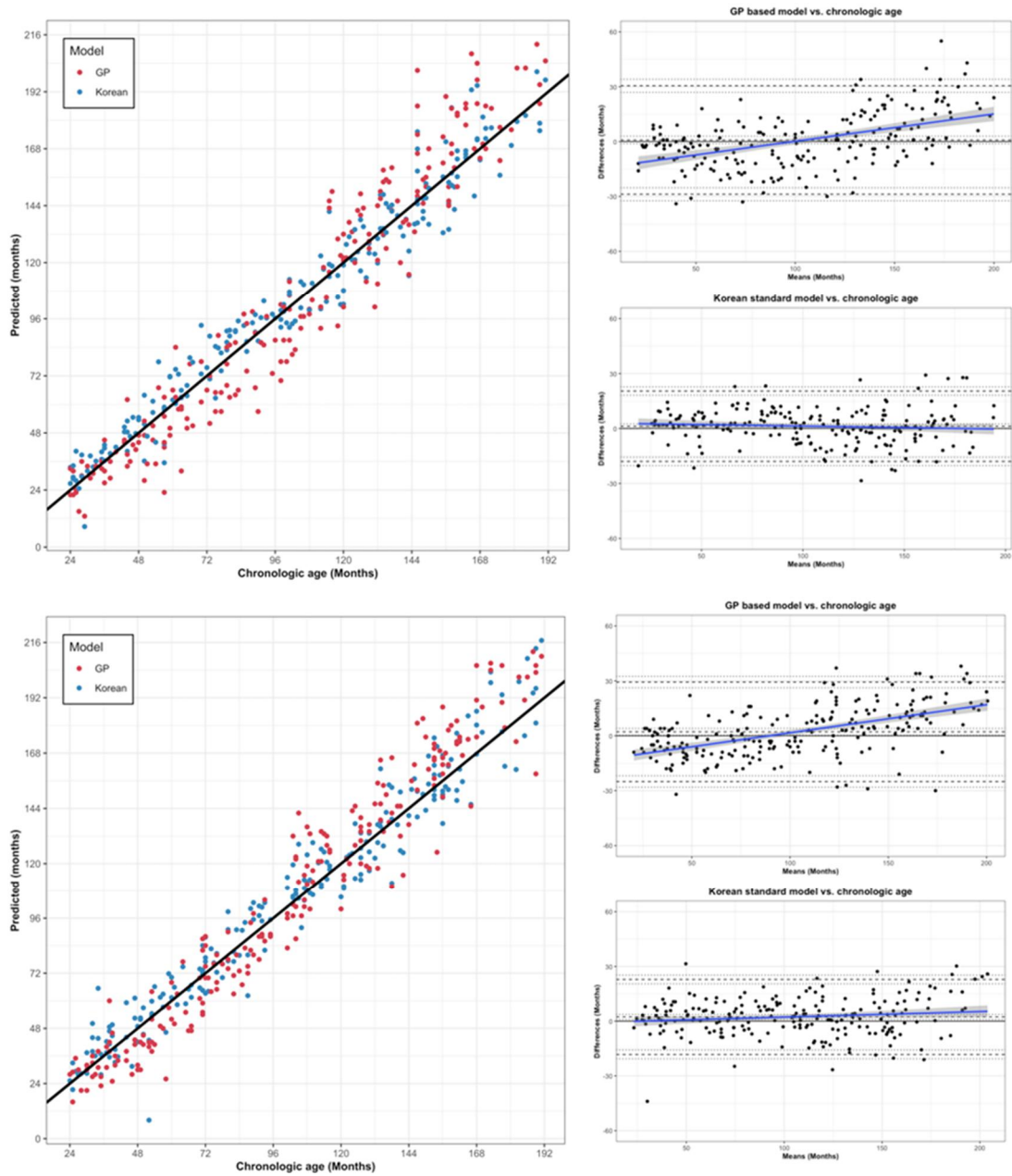
The results of subgroup analysis restricted to age 2–16 for male, and 2–14 for female are summarized in Table 3 and Figure 6. In both institutions, GP based model showed a systematic trend to underestimate the bone age before the age of 10 and to overestimate the bone after the age of 10 (Institution 1; slope, 0.15;  $P < .001$ ; Institution 2; slope, 0.15;  $P < .001$ ). Korean standard model also showed a systematic trend, but the slope was lower than GP based model (slope, 0.03;  $P = .048$ ). In addition, RMSE and MAE were lower in Korean standard model. Furthermore, the proportions of subjects with absolute differences  $\leq 6$ , 12, and 18 months were significantly higher in the Korean standard model in both institutions. The proportion of subjects with absolute differences  $\leq 24$  months was also higher in Institution 1, and statistical difference of that was not found only in Institution 2.

**Table 3.** Results of subgroup analysis restricted to age 2–16 for male, and 2–14 for female.

Parameters	Institution 1			Institution 2		
	GP	Korean	P-value	GP	Korean	P-value
RMSE (months)	12.2	9.8	<.001	10.7	10.1	<.001
MAE (months)	10.0	7.4	<.001	8.1	7.8	<.001
% of subjects with absolute difference						
≤ 6 months	36.1 (75/208)	51.0 (106/208)	.003	32.0 (70/219)	48.4 (106/219)	.001
≤ 12 months	62.5 (130/208)	79.3 (165/208)	<.001	65.8 (144/219)	76.7 (168/219)	.02
≤ 18 months	77.9 (162/208)	92.8 (193/208)	<.001	81.7 (179/219)	90.4 (198/219)	.01
≤ 24 months	90.9 (189/208)	97.1 (202/208)	.01	91.8 (201/219)	95.9 (210/219)	.11
Bland-Altman parameters						
Slope	0.15	-0.017	-	0.15	0.03	-
Intercept	-15	3	-	-14	-0.77	-
Bias	0.856	1.248	-	2.164	2.344	-
Standard deviation	15.137	9.804	-	13.849	10.477	-
95% limits of agreement	-28.8–30.5	-18.0–20.5	-	-25.0–29.3	-18.2–22.9	-
P-value <sup>a</sup>	<.001	.27	-	<.001	.048	-

RMSE = root mean square error; MAE = mean absolute error; GP = Greulich-Pyle

<sup>a</sup>P-value was calculated using the univariable linear regression analysis based on the Bland-Altman plot, with the independent variable as mean value of the chronologic age and predicted bone age and the dependent variable as difference between the chronologic age and predicted bone age.



**Figure 6.** Bivariate scatterplots showing association between chronologic age and predicted bone age by Greulich-Pyle (GP) based (red dots) and Korean based model (blue dots) and Bland-Altman plots showing a difference between the chronologic age and the predicted bone age in (A) Institution 1 and (B) Institution 2 datasets, restricted to age 2–16 for male, and 2–14 for female. Note that a systematic trend to underestimate the bone age before the age of 10 and to overestimate the bone after the age of 10 was reduced in Korean standard model compared to GP model (Institution 1; slope, 0.15 to -0.017;  $P < .001$  to .27; Institution 2; slope, 0.15 to 0.03;  $P < .001$  to .048).

*Korean Standard Atlas Development*

Using a Korean Standard model, Korean standard atlas was developed with the reference age of 0 to 24 months at 6-month intervals, and from 24 months to 19 years for boys and 18 years for girls at 1-year intervals (Appendix).

## DISCUSSION

In this study, we developed a deep learning model for prediction of bone age with a ground truth as chronological age derived from the contemporary healthy Korean pediatric population (i.e., Korean standard model). Compared to GP based model, Korean standard model showed a lower RMSE (10.2 vs. 12.4 months) and MAE (7.6 vs. 9.7 months), and the higher proportions of the subjects with absolute difference  $\leq 12$  months (69.5% vs. 77.2%) and  $\leq 18$  months (83.4% vs. 91.1%) in Institution 1. In addition, MAE of Korean standard model was lower (10.9 vs. 9.6 months) in Institution 2. The subgroup analysis restricted to age 2–16 for male and 2–14 for female also showed better prediction performance in Korean standard model. Furthermore, a systematic trend to underestimate the bone age before the age of 10 and to overestimate the bone age after the age of 10 was observed in GP based model. Therefore, our newly developed Korean standard model seems to be a feasible method reflecting a normal skeletal development of Korean pediatric population.

We affirmed the systemic bias when applying GP-based bone age prediction to Asian population based on approximately 20,000 radiographs from healthy Korean pediatric one. Zhang et al. reported that the bone age based on GP method was more advanced in Asian boys (11–15 years) and girls (10–13 years) compared to Caucasian (13). Ontell et al. also reported the delayed bone age in preadolescent period and advanced bone age in adolescent period for Asian boys (14). This systemic bias was reproduced from our data (underestimation of bone age before the age of 10, and overestimation of bone age after the age of 10). Considering the accuracy of deep learning-based bone age assessment system (9, 23), this trend was probably not derived from the performance of GP based model. Rather, this systemic trend is likely to be derived from different genetic factors, diet, and/or nutritional intakes between Korean and white pediatric population of upper socioeconomic level as a basis for the development of GP method. This indicates that skeletal maturation of contemporary Korean children and adolescents starts later and ends earlier than that of Caucasian. Obviously, this is an inevitable difference encountered in the real practice.

It should be emphasized that this systemic bias may affect the treatment decision. In general, delayed or advanced bone age is defined as the difference between bone age and chronologic age  $> 2SD$  of the mean (24). This could be roughly interpreted as a difference between bone

age and chronologic age of proximately higher than 12 months between 2 and 4 years of chronologic age, 18 months between 4 and 12 years, and 24 months after age 12 (25). In Institution 1, the proportions of the subjects with absolute difference  $\leq 12$  months and  $\leq 18$  months were significantly higher in Korean standard model. Furthermore, in the subgroup analysis restricted to the subjects with age 2–16 for male and 2–14 for female, the proportions of subjects with absolute differences  $\leq 6$ , 12, and 18 months were higher in Korean standard model in both institutions. Considering this, GP-based bone age prediction has a chance to lead an unnecessary diagnostic tests or treatments even in the healthy Korean children and adolescents. Our deep learning based Korean standard model demonstrated a potential to overcome this clinically significant bias. For this, further prospective studies to validate a clinical impact of Korean standard model in the real practice, especially in terms of ability to predict the eventual height after the end of skeletal maturation, are necessary.

Based on our newly developed Korean standard model, we developed a Korean Standard Atlas. In this atlas, in contrast to GP method with irregular intervals between the reference ages, intervals between the reference ages were regularized with the reference age of 0 to 24 months at 6-month intervals, and from 24 months to 19 years for boys and 18 years for girls at 1-year intervals. Notably, we selected the reference images to secure representativeness by (i) selection of the cases who showed the difference between the chronologic age and reference age less than 1 month; (ii) adaptation of GP method to affirm an appropriateness of bone maturation, together with the predicted bone age by Korean standard model; and (iii) consensus meeting manually reviewing the candidate images by four pediatric radiologists.

In 1996, a standard Korean bone age chart based on the TW2-20 score was developed using 3407 radiographs obtained from Korean children and adolescents (15). Compared to this, our model was developed based on a larger sample size with a narrower age range of the candidates in a specific reference age (e.g., in our model, the age range was restricted to 3 months [reference age  $\pm 1$  months]; however, in 1996 standard bone age chart, age range varied from 3 to 11 months). In addition, as a deep learning was applied, bone age can be predicted in a time-efficient and reproducible way. Therefore, we hope this model can be widely used in Korea.

There are several limitations of note. Firstly, the number of infants, toddlers, and older



adolescents in the training set were relatively small compared to the subject aged around 10. Therefore, the model might not be optimized in those ages. Indeed, both in the internal and external validation sets, the predicted bone age of the Korean standard model showed a wide dispersion from the chronologic age. It seems necessary to collect additional training dataset comprising infants, toddlers, and older adolescents in the future model modification. Secondly, although the chronologic age is used as the ground truth, the skeletal maturation can vary even with the same chronologic age (26). Lastly, we did not evaluate the performance of bone age assessment based on the newly introduced atlas.

In conclusion, a newly developed deep learning based Korean standard bone age assessment model to predict chronologic age showed a better performance than GP based bone age assessment model in healthy Korean children and adolescents, by reflecting a characteristic skeletal maturation in contemporary Korean children and adolescents. A Korean standard atlas of bone age based on a Korean standard model was newly introduced.

## REFERENCE LIST

1. Oh MS, Kim S, Lee J, Lee MS, Kim YJ, Kang KS. Factors associated with Advanced Bone Age in Overweight and Obese Children. *Pediatr Gastroenterol Hepatol Nutr* 2020;23:89-97
2. Kim D, Cho SY, Maeng SH, Yi ES, Jung YJ, Park SW, et al. Diagnosis and constitutional and laboratory features of Korean girls referred for precocious puberty. *Korean J Pediatr* 2012;55:481-486
3. Kelly PM, Diméglio A. Lower-limb growth: how predictable are predictions? *J Child Orthop* 2008;2:407-415
4. Creo AL, Schwenk WF, 2nd. Bone Age: A Handy Tool for Pediatric Providers. *Pediatrics* 2017;140
5. Greulich WW, Pyle SI, Todd TW, Brush Foundation C. *Radiographic Atlas of Skeletal Development of the Hand and Wrist*: Stanford University Press, 1950
6. Lee BD, Lee MS. Automated Bone Age Assessment Using Artificial Intelligence: The Future of Bone Age Assessment. *Korean J Radiol* 2021;22:792-800
7. Roche AF, Rohmann CG, French NY, Dávila GH. Effect of training on replicability of assessments of skeletal maturity (Greulich-Pyle). *Am J Roentgenol Radium Ther Nucl Med* 1970;108:511-515
8. Bull RK, Edwards PD, Kemp PM, Fry S, Hughes IA. Bone age assessment: a large scale comparison of the Greulich and Pyle, and Tanner and Whitehouse (TW2) methods. *Arch Dis Child* 1999;81:172-173
9. Kim JR, Shim WH, Yoon HM, Hong SH, Lee JS, Cho YA, et al. Computerized Bone Age Estimation Using Deep Learning Based Program: Evaluation of the Accuracy and Efficiency. *AJR Am J Roentgenol* 2017;209:1374-1380
10. Eng DK, Khandwala NB, Long J, Fefferman NR, Lala SV, Strubel NA, et al. Artificial Intelligence Algorithm Improves Radiologist Performance in Skeletal Age Assessment: A Prospective Multicenter Randomized Controlled Trial. *Radiology* 2021;301:692-699

11. Booz C, Yel I, Wichmann JL, Boettger S, Al Kamali A, Albrecht MH, et al. Artificial intelligence in bone age assessment: accuracy and efficiency of a novel fully automated algorithm compared to the Greulich-Pyle method. *Eur Radiol Exp* 2020;4:6
12. Alshamrani K, Messina F, Offiah AC. Is the Greulich and Pyle atlas applicable to all ethnicities? A systematic review and meta-analysis. *Eur Radiol* 2019;29:2910-2923
13. Zhang A, Sayre JW, Vachon L, Liu BJ, Huang HK. Racial differences in growth patterns of children assessed on the basis of bone age. *Radiology* 2009;250:228-235
14. Ontell FK, Ivanovic M, Ablin DS, Barlow TW. Bone age in children of diverse ethnicity. *AJR Am J Roentgenol* 1996;167:1395-1398
15. Yeon KM. Standard bone-age of infants and children in Korea. *J Korean Med Sci* 1997;12:9-16
16. King DG, Steventon DM, O'Sullivan MP, Cook AM, Hornsby VP, Jefferson IG, et al. Reproducibility of bone ages when performed by radiology registrars: an audit of Tanner and Whitehouse II versus Greulich and Pyle methods. *Br J Radiol* 1994;67:848-851
17. Mongan J, Moy L, Kahn CE, Jr. Checklist for Artificial Intelligence in Medical Imaging (CLAIM): A Guide for Authors and Reviewers. *Radiol Artif Intell* 2020;2:e200029
18. Kim JH, Yun S, Hwang SS, Shim JO, Chae HW, Lee YJ, et al. The 2017 Korean National Growth Charts for children and adolescents: development, improvement, and prospects. *Korean J Pediatr* 2018;61:135-149
19. He K, Zhang X, Ren S, Sun J. Deep Residual Learning for Image Recognition. 2016 IEEE Conference on Computer Vision and Pattern Recognition (CVPR) 2016 27-30 June 2016 [Epub]. <https://doi.org/10.1109/CVPR.2016.90:770-778>
20. Deng J, Dong W, Socher R, Li LJ, Kai L, Li F-F. ImageNet: A large-scale hierarchical image database. 2009 IEEE Conference on Computer Vision and Pattern Recognition 2009 20-25 June 2009 [Epub]. <https://doi.org/10.1109/CVPR.2009.5206848:248-255>
21. Gao B-B, Zhou H, Wu J, Geng X. Age Estimation Using Expectation of Label Distribution Learning. *IJCAI* 2018
22. Larson DB, Chen MC, Lungren MP, Halabi SS, Stence NV, Langlotz CP. Performance of a Deep-Learning Neural Network Model in Assessing Skeletal Maturity on Pediatric Hand Radiographs. *Radiology* 2018;287:313-322

23. Lea WW, Hong SJ, Nam HK, Kang WY, Yang ZP, Noh EJ. External validation of deep learning-based bone-age software: a preliminary study with real world data. *Sci Rep* 2022;12:1232
24. Martin DD, Wit JM, Hochberg Z, Sävendahl L, van Rijn RR, Fricke O, et al. The use of bone age in clinical practice - part 1. *Horm Res Paediatr* 2011;76:1-9
25. Diagnostic approach to children and adolescents with short stature. Web site. <https://www.uptodate.com/contents/diagnostic-approach-to-children-and-adolescents-with-short-stature#!%3Fmsclkid=ee1b944dba4211ec9a6827f36edc65af>. Accessed Apr 12, 2022,
26. Gilsanz V, Ratib O. *Hand Bone Age: A Digital Atlas of Skeletal Maturity*: Springer Berlin Heidelberg, 2011

## 국문요약

**목적:** 건강한 한국 아동 및 청소년의 손 방사선 사진을 이용한 딥 러닝 기반 골연령 예측 모델을 개발 및 Greulich-Pyle 방식의 딥 러닝 기반 골연령 예측 모델 (GP 기반 모델)과 비교함으로써 검증하고, 한국 표준 아틀라스를 개발하고자 하였다.

**대상 및 방법:** 1998년에서 2019년에 서울아산병원에서 골발달이 정상일 것으로 추정되는 한국 아동 및 청소년의 손 방사선 사진 21,036장을 이용하여 역연령을 예측하도록 컨볼루션 신경망 (한국 표준 모델)을 훈련하였다. 외적 타당성을 검증하기 위해 부산대학교 양산병원 (기관 1, n=304) 및 단국대학교 병원 (기관 2, n=314)에서 얻어진 두 개의 검토군을 각각 사용하였다. 평균절대오차 (mean absolute error; MAE), 평균 제곱근편차 (root mean square error; RMSE), 역연령과 예측 골연령의 차이가 6, 12, 18 및 24개월 내인 대상의 분율을 GP 기반 모델과 비교하였다. Bland-Altman 분석을 추가로 수행하였으며, 남아에서 2-16세, 여아에서 2-14세로 제한한 하위 그룹 분석을 추가 수행하였다.

**결과:** 한국 표준 모델은 GP 기반 모델에 비해, 기관 1에서 RMSE (10.2 vs. 12.4개월;  $P<.001$ ), MAE (7.6 vs. 9.7개월;  $P<.001$ )가 낮았고 역연령과 골연령 차이가 12개월 이내 ( $P<.04$ ), 18개월 이내인 경우의 분율도 더 높았다 ( $P<.007$ ). 기관 2에서는 한국 표준모형의 MAE가 낮았다 (10.9 vs. 9.6개월;  $P<.008$ ). 하위 그룹 분석에서 기관 1, 2 모두에서 낮은 한국 표준 모델이 RMSE, MAE가 낮았고 (모두  $P<.001$ ) 역연령-골연령 차이가 6, 12 및 18개월 내인 경우의 분율이 더 높았다 (모두  $P<.05$ ). 또한 GP 기반 모델에서 보이는 전반적인 경향차가 한국 표준 모델에서 감소하였다 (기관 1,  $P<.001$ 에서 .27로; 기관 2,  $P<.001$ 에서 .048로). 한국 표준 아틀라스는 한국 표준 모델에 근거하여 합의 회의를 통해 개발 및 완성되었다.

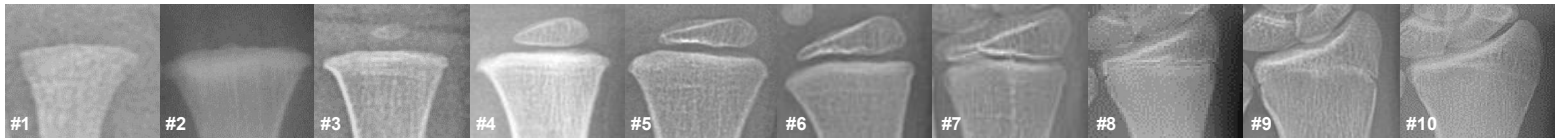
**결론:** 딥러닝 기반의 한국 표준 골연령 평가 모델은 건강한 한국 아동 및 청소년의 특징적인 골성숙과정을 반영함으로써 GP 기반 골연령 평가 모델보다 더 나은 성능을 보였다. 한국 표준 모델을 대표하는 한국 표준 아틀라스를 새롭게 제작하였다.

# **Korean Standard Atlas**

**MALE**

# Male standard

## Radius



Timepoint	Age	Major changes
#1	Newborn	-
#2	1 year	Flaring at the end is pronounced.
#3	1 year 6 months	Center of ossification is now visible.
#4	3 years	The epiphysis of the radius has become wedge-shaped.
#5	5 years	The volar and dorsal surfaces of the epiphysis can now be distinguished.
#6	6 years	The distal margin of the ulnar tip of the radial epiphysis has flattened slightly.
#7	12 years	The epiphysis is as wide as the adjacent border of the shaft.
#8	15 years	The epiphysis has capped its shaft.
#9	16 years	Epiphyseal-diaphyseal fusion has begun.
#10	19 years	The radial epiphyseal line has been almost eliminated.

# Male standard

## Ulna

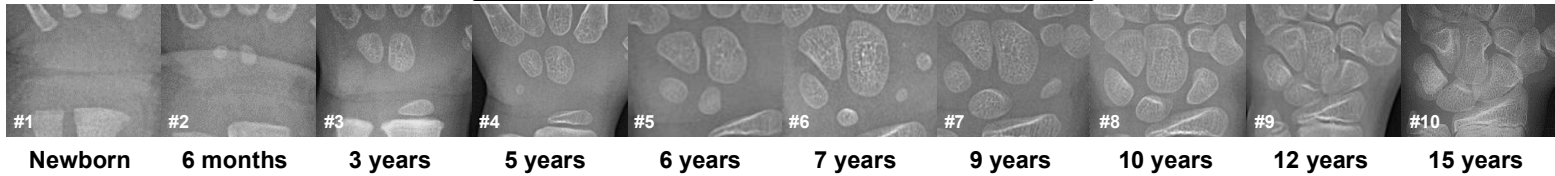


Timepoint	Age	Major changes
#1	Newborn	-
#2	1 year	Flaring at the end is pronounced.
#3	9 years	The ossification center is now visible.
#4	11 years	The epiphysis has widened and thickened. Note that there is a slight indentation in the distal surface.
#5	14 years	The growth cartilage plates are uniformly narrow. The ulnar styloid process is pronounced.
#6	15 years	The epiphysis is now as wide as its shaft.
#7	16 years	Epiphyseal-diaphyseal fusion has begun.
#8	18 years	Epiphyseal-diaphyseal fusion has been completed.



# Male standard

## Carpal bones



Timepoint	Age	Major changes
#1	Newborn	-
#2	6 months	Ossification centers of the capitate and hamate are visible.
#3	3 years	The capitate and hamate have increased further in size.
#4	5 years	<ul style="list-style-type: none"> <li>The ossification center of the triquetrum is visible.</li> <li>The concavity in the margin of the capitate adjacent to the hamate suggests the beginning of the reciprocal shaping.</li> </ul>
#5	6 years	The ossification center of the lunate is now well visible.
#6	7 years	<ul style="list-style-type: none"> <li>The ossification centers of trapezium, trapezoid, and scaphoid are now visible.</li> </ul>
#7	9 years	<ul style="list-style-type: none"> <li>The distinct curved radiopaque line at the distal margin of the lunate becomes evident.</li> <li>The metacarpal margin of the hamate is distinctly flattened.</li> <li>The surface of the trapezoid adjacent to the capitate has begun to be flattened.</li> </ul>
#8	10 years	<ul style="list-style-type: none"> <li>The spaces between the capitate and lunate, and lunate and radial epiphysis have been reduced.</li> <li>The radiopaque lines adjacent to the metacarpal surface of the hamate, capitate, and trapezoid are visible.</li> </ul>
#9	12 years	<ul style="list-style-type: none"> <li>Reciprocal shaping has progressed in all the carpals.</li> <li>The capitate surface of the scaphoid now overlaps the adjacent portion of the capitate.</li> </ul>
#10	15 years	A part of the outline of the tubercle of the scaphoid is now seen.

# Male standard

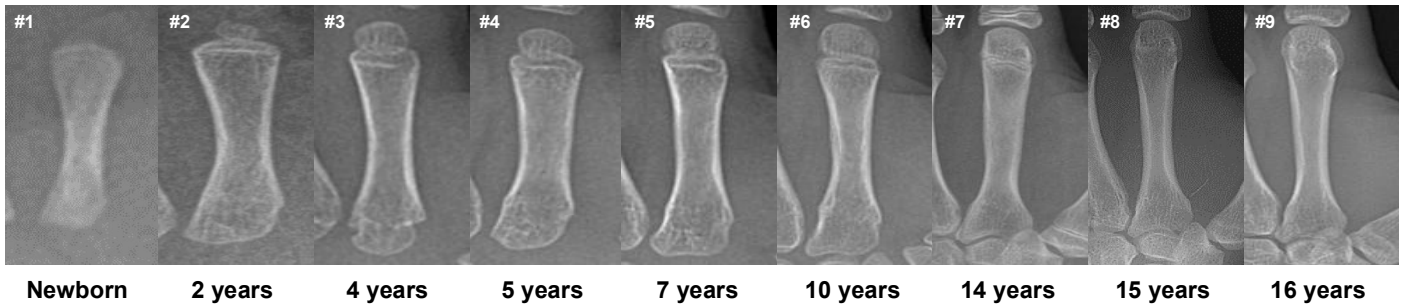
## 1<sup>st</sup> metacarpal



Timepoint	Age	Major changes
#1	Newborn	-
#2	3 years	The epiphysis is now visible.
#3	6 years	The epiphysis has increased further in size.
#4	10 years	Reciprocal shaping of the epiphysis has progressed.
#5	13 years	The ossification center of the sesamoid in the tendon of the adduct pollicis is now evident.
#6	15 years	Fusion has been advanced.
#7	17 years	The epiphyseal lines have been further disappeared.
#8	19 years	The epiphyseal lines have been further disappeared.

# Male standard

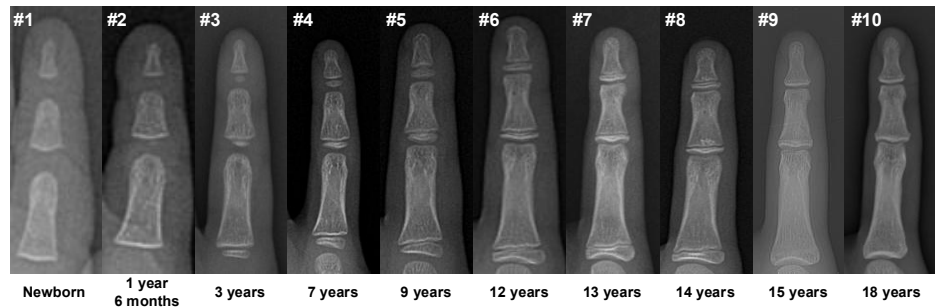
## 2<sup>nd</sup> metacarpal



Timepoint	Age	Major changes
#1	Newborn	-
#2	2 years	Center of ossification is now visible.
#3	4 years	The epiphysis has increased further in size.
#4	5 years	The surface of the base of the 2 <sup>nd</sup> metacarpal is now flattened.
#5	7 years	The base of the 2 <sup>nd</sup> metacarpal is now distinctly indented.
#6	10 years	The concavity in the base of the 2 <sup>nd</sup> metacarpal has become more pronounced.
#7	14 years	The growth cartilage plate has been narrowed.
#8	15 years	Epiphyseal-diaphyseal fusion has been advanced.
#9	16 years	Epiphyseal-diaphyseal fusion has been completed.

# Male standard

## 2<sup>nd</sup> phalanx



Timepoint	Age	Major changes
#1	Newborn	-
#2	1 year 6 months	Centers of ossifications are now visible.
#3	3 years	The epiphysis of the middle phalanx has been shown as disc-like structures which are thickest in the middle and taper toward each end.
#4	7 years	The epiphysis of the proximal phalanx is now somewhat wedge-shaped, tapering toward the ulnar end.
#5	9 years	The distal end of the proximal phalanx has become slightly concave.
#6	12 years	The epiphysis of the proximal phalanx is as wide as its shaft.
#7	13 years	The epiphysis of the distal phalanx is beginning to conform in shape to that of the respective middle phalanx.
#8	14 years	The epiphysis of phalanx has now begun to cap its shaft.
#9	15 years	Fusion has been partially completed in some epiphyses.
#10	18 years	The epiphyseal lines have been nearly disappeared.

## Male standard

Age: newborn



Target bones	Major changes
Radius	-
Ulna	-
Carpal bone	-
1 <sup>st</sup> metacarpal	-
Other metacarpals	-
Phalanges	-

## Male standard

Age: 6 months



Target bones	Major changes
Radius	-
Ulna	-
Carpal bone	Ossification centers of the capitate and hamate are visible.
1 <sup>st</sup> metacarpal	-
Other metacarpals	-
Phalanges	-

## Male standard

Age: 1 year



Target bones	Major changes
Radius	Flaring at the end is pronounced.
Ulna	Flaring at the end is pronounced.
Carpal bone	Increase in size of the capitate and hamate has brought these more closely together.
1 <sup>st</sup> metacarpal	-
Other metacarpals	-
Phalanges	-

## Male standard

Age: 1 year 6 months



Target bones	Major changes
Radius	Center of ossification is now visible.
Ulna	-
Carpal bone	The flattening of the hamate surface of the capitate has occurred.
1 <sup>st</sup> metacarpal	-
Other metacarpals	-
Phalanges	Multiple centers of ossifications are now visible.



## Male standard

Age: 2 years



Target bones	Major changes
Radius	The ulnar side of the radial epiphysis is pointed and its radial side is thicker and convex.
Ulna	-
Carpal bone	The flattening of the hamate surface of the capitate is now more pronounced.
1 <sup>st</sup> metacarpal	-
Other metacarpals	Center of ossification is now visible.
Phalanges	-

## Male standard

Age: 3 years



Target bones	Major changes
Radius	The epiphysis of the radius has become wedge-shaped.
Ulna	-
Carpal bone	The capitate and hamate have increased further in size.
1 <sup>st</sup> metacarpal	The epiphysis is now visible.
Other metacarpals	The epiphysis has increased further in size.
Phalanges	<ul style="list-style-type: none"><li>The epiphyses of the 5<sup>th</sup> finger are visible.</li><li>Epiphyses of the middle phalanges of the 2<sup>nd</sup>, 3<sup>rd</sup>, and 4<sup>th</sup> fingers have been shown as disc-like structures which are thickest in the middle and taper toward each end.</li></ul>

## Male standard

Age: 4 years



Target bones	Major changes
Radius	-
Ulna	-
Carpal bone	The ossification center of the triquetrum seems to be now visible.
1 <sup>st</sup> metacarpal	-
Other metacarpals	-
Phalanges	-

## Male standard

Age: 5 years



Target bones	Major changes
Radius	The volar and dorsal surfaces of the epiphysis can now be distinguished.
Ulna	-
Carpal bone	<ul style="list-style-type: none"><li>• The ossification centers of the triquetral has grown larger.</li><li>• The concavity in the margin of the capitate adjacent to the hamate suggests the beginning of the reciprocal shaping.</li></ul>
1 <sup>st</sup> metacarpal	-
Other metacarpals	The surface of the base of the 2 <sup>nd</sup> metacarpal is now flattened.
Phalanges	-

## Male standard

Age: 6 years



Target bones	Major changes
Radius	The distal margin of the ulnar tip of the radial epiphysis has flattened slightly.
Ulna	-
Carpal bone	The ossification center of the lunate is now well visible.
1 <sup>st</sup> metacarpal	The epiphysis has increased further in size.
Other metacarpals	The epiphysis has increased further in size.
Phalanges	-

## Male standard

Age: 7 years



Target bones	Major changes
Radius	-
Ulna	-
Carpal bone	<ul style="list-style-type: none"><li>• The ossification centers of trapezium, trapezoid, and scaphoid are now visible.</li><li>• Both a lunar and a hamate facet can now be distinguished on the triquetral.</li></ul>
1 <sup>st</sup> metacarpal	-
Other metacarpals	The base of the 2 <sup>nd</sup> metacarpal is now distinctly indented.
Phalanges	The epiphyses of the proximal phalanges of the 2 <sup>nd</sup> and 3 <sup>rd</sup> fingers are now somewhat wedge-shaped, tapering toward their ulnar ends.

## Male standard

Age: 8 years



Target bones	Major changes
Radius	-
Ulna	-
Carpal bone	The ossification centers of trapezium, trapezoid, and scaphoid are further enlarged.
1 <sup>st</sup> metacarpal	-
Other metacarpals	-
Phalanges	The epiphyses of the distal phalanges of the 2 <sup>nd</sup> to 5 <sup>th</sup> fingers are as wide as their shafts.

# Male standard

Age: 9 years



Target bones	Major changes
Radius	-
Ulna	The ossification center is now visible.
Carpal bone	<ul style="list-style-type: none"><li>• The distinct curved radiopaque line at the distal margin of the lunate becomes evident.</li><li>• The surface of the trapezium adjacent to the 1<sup>st</sup> metacarpal has begun to flatten.</li><li>• The metacarpal margin of the hamate is now distinctly flattened.</li><li>• The surface of the trapezoid adjacent to the capitate has begun to be flattened.</li></ul>
1 <sup>st</sup> metacarpal	-
Other metacarpals	-
Phalanges	<ul style="list-style-type: none"><li>• The distal ends of the 2<sup>nd</sup> and 3<sup>rd</sup> proximal phalanges have become slightly concave.</li></ul>



## Male standard

Age: 10 years



Target bones	Major changes
Radius	-
Ulna	-
Carpal bone	<ul style="list-style-type: none"><li>• The spaces between the hamate and triquetrum, capitate and lunate, and lunate and radial epiphysis have been further reduced.</li><li>• The radiopaque lines adjacent to the metacarpal surface of the hamate, capitate, and trapezoid mark a part of their respective volar margins.</li></ul>
1 <sup>st</sup> metacarpal	Reciprocal shaping of the epiphysis has progressed.
Other metacarpals	The concavity in the base of the 2 <sup>nd</sup> metacarpal has become more pronounced.
Phalanges	-

## Male standard

Age: 11 years



Target bones	Major changes
Radius	-
Ulna	The epiphysis has widened and thickened. Note that there is a slight indentation in the distal surface.
Carpal bone	The two metacarpal articular surfaces of the capitate are beginning to differentiate.
1 <sup>st</sup> metacarpal	-
Other metacarpals	-
Phalanges	-

## Male standard

Age: 12 years



Target bones	Major changes
Radius	The epiphysis is as wide as the adjacent border of the shaft.
Ulna	-
Carpal bone	<ul style="list-style-type: none"><li>• Reciprocal shaping has progressed in all the carpals.</li><li>• The capitate surface of the scaphoid now overlaps the adjacent portion of the capitate.</li><li>• The outline of the hook of the hamate is now visible.</li></ul>
1 <sup>st</sup> metacarpal	-
Other metacarpals	-
Phalanges	The epiphyses of the proximal phalanges of the 2 <sup>nd</sup> to 5 <sup>th</sup> fingers are as wide as their shafts.

## Male standard

Age: 13 years



Target bones	Major changes
Radius	The developing styloid process of the radial epiphysis has become more distinct. The radiopaque line adjacent to the cartilage plate now extends farther laterally.
Ulna	-
Carpal bone	Reciprocal shaping has progressed in all the carpals.
1 <sup>st</sup> metacarpal	The ossification center of the sesamoid in the tendon of the adduct pollicis is now evident.
Other metacarpals	-
Phalanges	The epiphyses of the distal phalanges of the 2 <sup>nd</sup> to 4 <sup>th</sup> fingers are beginning to conform in shape to that of the trochlear surfaces of their respective middle phalanges.

## Male standard

Age: 14 years



Target bones	Major changes
Radius	<ul style="list-style-type: none"><li>• The epiphysis have now begun to cap the shaft.</li><li>• The growth cartilage plates are uniformly narrow.</li></ul>
Ulna	The growth cartilage plates are uniformly narrow.
Carpal bone	-
1 <sup>st</sup> metacarpal	-
Other metacarpals	-
Phalanges	<ul style="list-style-type: none"><li>• The epiphyses of the proximal phalanges of the 2<sup>nd</sup> to 5<sup>th</sup> fingers have increased in thickness and their radial margins end in distally directed tips.</li><li>• The epiphyses of phalanges of the 2<sup>nd</sup> to 5<sup>th</sup> fingers have now begun to cap their shafts.</li></ul>

## Male standard

Age: 15 years



Target bones	Major changes
Radius	The epiphysis has capped its shaft.
Ulna	The epiphysis is now as wide as its shaft.
Carpal bone	A part of the outline of the tubercle of the scaphoid is now seen.
1 <sup>st</sup> metacarpal	Fusion has been advanced.
Other metacarpals	Fusion has been partially completed in some epiphyses.
Phalanges	Fusion has been partially completed in some epiphyses.

## Male standard

Age: 16 years



Target bones	Major changes
Radius	Epiphyseal-diaphyseal fusion has begun.
Ulna	Epiphyseal-diaphyseal fusion has begun.
Carpal bone	-
1 <sup>st</sup> metacarpal	-
Other metacarpals	Epiphyseal-diaphyseal fusion has been completed.
Phalanges	Epiphyseal-diaphyseal fusion has been further advanced.

## Male standard

Age: 17 years



Target bones	Major changes
Radius	Epiphyseal-diaphyseal fusion has been further advanced.
Ulna	Epiphyseal-diaphyseal fusion has been further advanced.
Carpal bone	-
1 <sup>st</sup> metacarpal	The epiphyseal lines have been further disappeared.
Other metacarpals	-
Phalanges	The epiphyseal lines have been further disappeared.



## Male standard

Age: 18 years



Target bones	Major changes
Radius	The epiphyseal lines have been further disappeared.
Ulna	Epiphyseal-diaphyseal fusion has been completed.
Carpal bone	-
1 <sup>st</sup> metacarpal	-
Other metacarpals	-
Phalanges	The epiphyseal lines have been nearly disappeared.

## Male standard

Age: 19 years



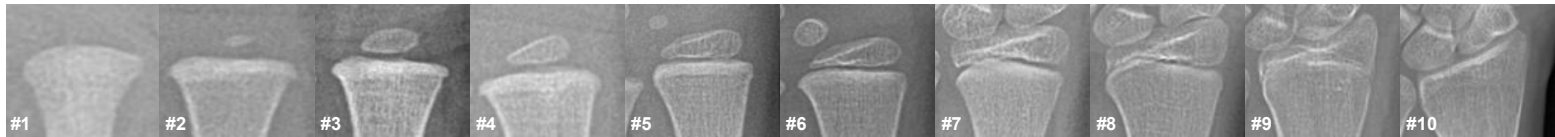
Target bones	Major changes
Radius	The radial epiphyseal line has been almost eliminated.
Ulna	-
Carpal bone	-
1 <sup>st</sup> metacarpal	The epiphyseal lines have been further disappeared.
Other metacarpals	-
Phalanges	-

# **Korean Standard Atlas**

## **FEMALE**

# Female standard

## Radius



Timepoint	Age	Major changes
#1	Newborn	-
#2	1 year	<ul style="list-style-type: none"> <li>• Flaring at the end is pronounced.</li> <li>• A small center of ossification is visible.</li> </ul>
#3	1 year 6 months	A center of ossification has increased further in size.
#4	2 years	The epiphysis of the radius has become wedge-shaped.
#5	4 years	The volar and dorsal surfaces of the epiphysis can now be distinguished.
#6	5 years	The distal margin of the ulnar tip of the radial epiphysis has flattened slightly.
#7	10 years	The epiphysis is as wide as the adjacent border of the shaft.
#8	11 years	<ul style="list-style-type: none"> <li>• The developing styloid process of the radial epiphysis has become more distinct.</li> <li>• The epiphysis has now begun to cap the shaft.</li> </ul>
#9	14 years	Epiphyseal-diaphyseal fusion has begun.
#10	18 years	The epiphyseal line has been nearly disappeared.

# Female standard

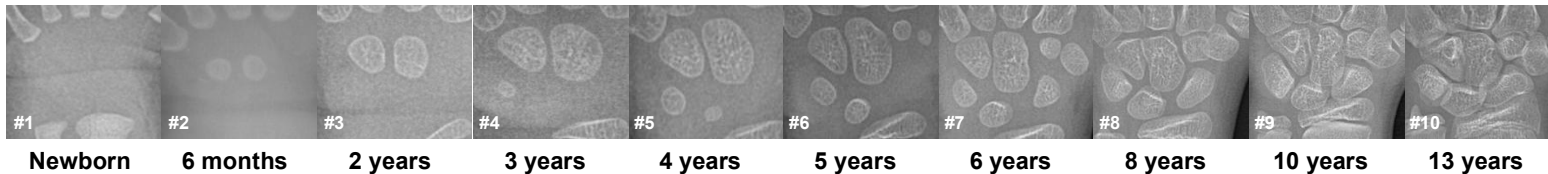
## Ulna



Timepoint	Age	Major changes
#1	Newborn	-
#2	1 year	Flaring at the end is pronounced.
#3	7 years	The ossification center is now visible.
#4	10 years	The epiphysis has widened and thickened. Note that there is a slight indentation in the distal surface.
#5	11 years	The ulnar styloid process is pronounced.
#6	12 years	The growth cartilage plate is uniformly narrow.
#7	15 years	Epiphyseal-diaphyseal fusion has begun.
#8	18 years	Epiphyseal-diaphyseal fusion has been completed.

# Female standard

## Carpal bones



Timepoint	Age	Major changes
#1	Newborn	-
#2	6 months	Ossification centers of the capitate and hamate are visible.
#3	2 years	The capitate and hamate have increased further in size.
#4	3 years	<ul style="list-style-type: none"> <li>The ossification center of the triquetral is visible.</li> <li>The concavity in the margin of the capitate adjacent to the hamate suggests the beginning of the reciprocal shaping.</li> </ul>
#5	4 years	The ossification center of the lunate is visible.
#6	5 years	<ul style="list-style-type: none"> <li>The ossification centers of trapezium and trapezoid are visible.</li> <li>The distinct curved radiopaque line at the distal margin of the lunate is now visible.</li> </ul>
#7	6 years	<ul style="list-style-type: none"> <li>The ossification centers of the scaphoid is visible.</li> <li>The ossification centers of trapezium and trapezoid has increased further in size.</li> </ul>
#8	8 years	The radiopaque lines adjacent to the metacarpal surface of the hamate, capitate, and trapezoid mark a part of their respective volar margins.
#9	10 years	The carpal bones became larger, showing increase in the degree of reciprocal shaping.
#10	13 years	A part of the outline of the tubercle of the scaphoid is now seen.

# Female standard

## 1<sup>st</sup> metacarpal



Timepoint	Age	Major changes
#1	Newborn	-
#2	2 years	The epiphysis is now visible.
#3	6 years	The epiphysis has increased further in size.
#4	9 years	Reciprocal shaping of the epiphysis has progressed.
#5	11 years	The ossification center of the sesamoid in the tendon of the adduct pollicis is now evident.
#6	12 years	Epiphyseal-diaphyseal fusion has begun.
#7	13 years	Epiphyseal-diaphyseal fusion becomes evident.
#8	18 years	The epiphyseal lines have been further disappeared.

# Female standard

## 2<sup>nd</sup> metacarpal

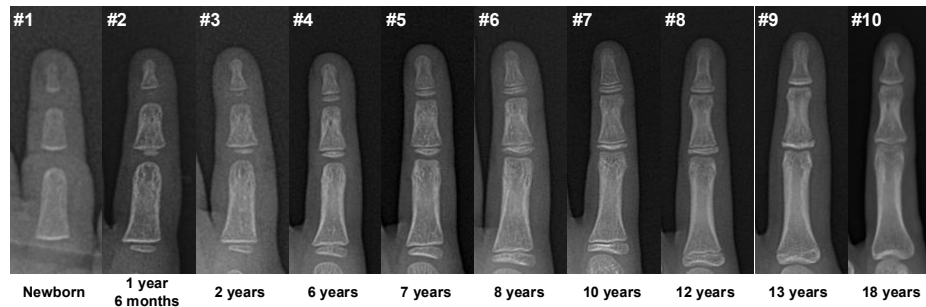


Timepoint	Age	Major changes
#1	Newborn	-
#2	1 year 6 months	Center of ossification is now visible.
#3	2 years	The epiphysis has increased further in size.
#4	4 years	The surface of the base is now flattened.
#5	7 years	The base is now distinctly indented.
#6	9 years	The concavity of the base has become more pronounced.
#7	13 years	Epiphyseal-diaphyseal fusion has begun.
#8	15 years	Epiphyseal-diaphyseal fusion has been advanced.
#9	16 years	The epiphyseal line of the phalanx has been further disappeared.



# Female standard

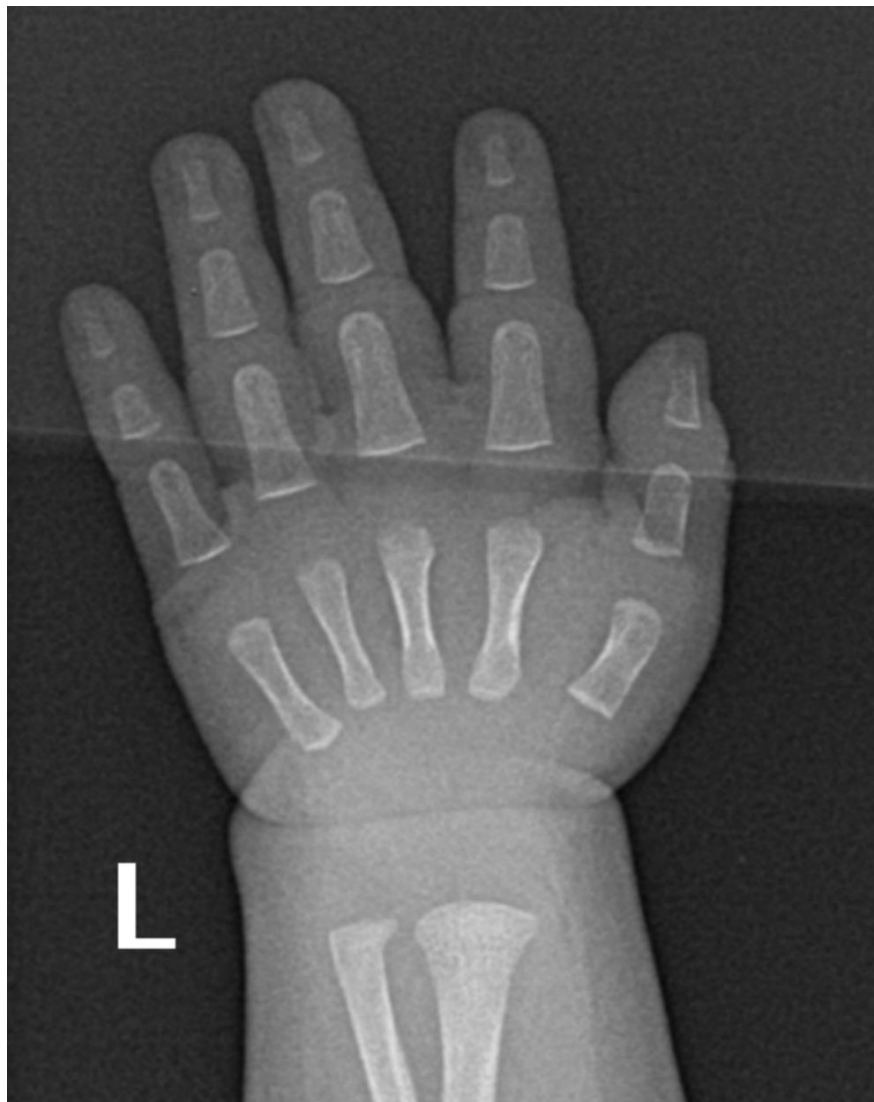
## 2<sup>nd</sup> phalanx



Timepoint	Age	Major changes
#1	Newborn	-
#2	1 year 6 months	Centers of ossifications are now visible.
#3	2 years	The epiphysis of the middle phalanx has been shown as disc-like structures which are thickest in the middle and taper toward each end.
#4	6 years	The epiphysis of the proximal phalanx is now somewhat wedge-shaped, tapering toward the ulnar end.
#5	7 years	The distal end of the proximal phalanx has become slightly concave.
#6	8 years	The epiphysis of the proximal phalanx is as wide as its shaft.
#7	10 years	The epiphysis of the distal phalanx is beginning to conform in shape to that of the respective middle phalanx.
#8	12 years	The epiphysis of phalanx has now begun to cap its shaft.
#9	13 years	Fusion has been partially completed in some epiphyses.
#10	18 years	The epiphyseal lines have been nearly disappeared.

## Female standard

Age: newborn



Target bones	Major changes
Radius	-
Ulna	-
Carpal bone	-
1 <sup>st</sup> metacarpal	-
Other metacarpals	-
Phalanges	-

## Female standard

Age: 6 months



Target bones	Major changes
Radius	-
Ulna	-
Carpal bone	Ossification centers of the capitate and hamate are visible.
1 <sup>st</sup> metacarpal	-
Other metacarpals	-
Phalanges	-

# Female standard

Age: 1 year



Target bones	Major changes
Radius	<ul style="list-style-type: none"><li>• Flaring at the end is pronounced.</li><li>• A small center of ossification is visible.</li></ul>
Ulna	Flaring at the end is pronounced.
Carpal bone	Increase in size of the capitate and hamate has brought these more closely together.
1 <sup>st</sup> metacarpal	-
Other metacarpals	-
Phalanges	Centers of ossification in 2 <sup>nd</sup> and 3 <sup>rd</sup> proximal phalanges, and 1 <sup>st</sup> distal phalanx are visible.

## Female standard

Age: 1 year 6 months



Target bones	Major changes
Radius	A center of ossification has increased further in size.
Ulna	-
Carpal bone	-
1 <sup>st</sup> metacarpal	-
Other metacarpals	Center of ossification in the head of 2 <sup>nd</sup> metacarpal is now visible.
Phalanges	Multiple centers of ossifications are now visible.

## Female standard

Age: 2 years



Target bones	Major changes
Radius	The epiphysis of the radius has become wedge-shaped.
Ulna	-
Carpal bone	The capitate and hamate have increased further in size.
1 <sup>st</sup> metacarpal	A small center of ossification is visible.
Other metacarpals	Centers of ossification are more pronounced.
Phalanges	<ul style="list-style-type: none"><li>Centers of ossifications are more pronounced.</li><li>Epiphyses of the middle phalanges have been shown as disc-like structures which are thickest in the middle and taper toward each end.</li></ul>

## Female standard

Age: 3 years



Target bones	Major changes
Radius	-
Ulna	-
Carpal bone	<ul style="list-style-type: none"><li>• The ossification center of the triquetrum is visible.</li><li>• The concavity in the margin of the capitate adjacent to the hamate suggests the beginning of the reciprocal shaping.</li></ul>
1 <sup>st</sup> metacarpal	Center of ossification is more pronounced.
Other metacarpals	Centers of ossification are more pronounced.
Phalanges	-

# Female standard

**Age: 4 years**



Target bones	Major changes
Radius	The volar and dorsal surfaces of the radial epiphysis is now distinguished.
Ulna	-
Carpal bone	<ul style="list-style-type: none"><li>• The ossification center of the lunate is visible.</li><li>• The ossification center of the triquetral has increased further in size.</li></ul>
1 <sup>st</sup> metacarpal	-
Other metacarpals	The surface of the base of the 2 <sup>nd</sup> metacarpal has begun to flatten.
Phalanges	-



## Female standard

Age: 5 years



Target bones	Major changes
Radius	The distal margin of the ulnar tip of the radial epiphysis has flattened slightly.
Ulna	-
Carpal bone	<ul style="list-style-type: none"><li>• The ossification centers of trapezium and trapezoid are visible.</li><li>• The distinct curved radiopaque line at the distal margin of the lunate is now visible.</li></ul>
1 <sup>st</sup> metacarpal	-
Other metacarpals	-
Phalanges	-

## Female standard

Age: 6 years



Target bones	Major changes
Radius	-
Ulna	-
Carpal bone	<ul style="list-style-type: none"><li>• The ossification centers of the scaphoid is visible.</li><li>• The ossification centers of trapezium and trapezoid has increased further in size.</li></ul>
1 <sup>st</sup> metacarpal	The epiphysis has increased further in size.
Other metacarpals	-
Phalanges	The epiphyses of the proximal phalanx are now somewhat wedge-shaped, tapering toward their ulnar ends.

## Female standard

Age: 7 years



Target bones	Major changes
Radius	-
Ulna	The ossification center in the ulnar epiphysis is visible.
Carpal bone	<ul style="list-style-type: none"><li>• The surface of trapezium adjacent the 1<sup>st</sup> metacarpal has begun to flatten.</li><li>• The metacarpal margin of the hamate is distinctly flattened.</li><li>• The surface of the trapezoid adjacent to the capitate has begun to flatten.</li></ul>
1 <sup>st</sup> metacarpal	-
Other metacarpals	The base of the 2 <sup>nd</sup> metacarpal is now distinctly indented.
Phalanges	The distal ends of the 2 <sup>nd</sup> and 3 <sup>rd</sup> proximal phalanges have become slightly concave.

## Female standard

Age: 8 years



Target bones	Major changes
Radius	-
Ulna	The epiphysis has widened and thickened.
Carpal bone	The radiopaque lines adjacent to the metacarpal surface of the hamate, capitate, and trapezoid mark a part of their respective volar margins.
1 <sup>st</sup> metacarpal	The epiphysis is as wide as the adjacent borders of their shafts.
Other metacarpals	The concavity in the base of 2 <sup>nd</sup> metacarpal adjacent to the trapezoid has become more pronounced.
Phalanges	The epiphyses of the proximal phalanges are as wide as the adjacent borders of their shafts.

# Female standard

Age: 9 years



Target bones	Major changes
Radius	-
Ulna	-
Carpal bone	<ul style="list-style-type: none"><li>• The spaces between the capitate and lunate, and lunate and radial epiphysis have been further reduced.</li><li>• The two metacarpal articular surfaces of the capitate are beginning to differentiate.</li><li>• The capitate surface of the scaphoid now overlaps the adjacent portion of the capitate.</li><li>• The outline of the hook of the hamate is now visible.</li></ul>
1 <sup>st</sup> metacarpal	Reciprocal shaping of the epiphysis has progressed.
Other metacarpals	The concavity in the base of the 2 <sup>nd</sup> metacarpal has become more pronounced.
Phalanges	-

## Female standard

Age: 10 years



Target bones	Major changes
Radius	-
Ulna	-
Carpal bone	<ul style="list-style-type: none"><li>• The carpal bones became larger, showing increase in the degree of reciprocal shaping.</li><li>• The capitate surface of the scaphoid now overlaps the adjacent portion of the capitate.</li></ul>
1 <sup>st</sup> metacarpal	-
Other metacarpals	The epiphyses are as wide as the adjacent margins of their shafts.
Phalanges	The epiphyses of the distal phalanges of the 2 <sup>nd</sup> to 4 <sup>th</sup> fingers are beginning to conform in shape to that of the trochlear surfaces of their respective middle phalanges.

## Female standard

Age: 11 years



Target bones	Major changes
Radius	<ul style="list-style-type: none"><li>• The developing styloid process of the radial epiphysis has become more distinct.</li><li>• The epiphysis has now begun to cap the shaft.</li></ul>
Ulna	The ulnar styloid process is more pronounced.
Carpal bone	-
1 <sup>st</sup> metacarpal	The ossification center of the sesamoid in the tendon of the adduct pollicis is now evident.
Other metacarpals	-
Phalanges	-

## Female standard

Age: 12 years



Target bones	Major changes
Radius	The growth cartilage plate is uniformly narrow.
Ulna	<ul style="list-style-type: none"><li>• The growth cartilage plate is uniformly narrow.</li><li>• Some portions of the epiphyseal-shaft spaces are fuzzy.</li><li>• The epiphysis of the ulna is as wide as its shaft.</li></ul>
Carpal bone	-
1 <sup>st</sup> metacarpal	Epiphyseal-diaphyseal fusion has begun.
Other metacarpals	-
Phalanges	The epiphyses of phalanges have begun to cap their shafts. In the proximal phalanges, the capping is more clearly visible on the radial than on the ulnar sides of the epiphyses.



## Female standard

Age: 13 years



Target bones	Major changes
Radius	-
Ulna	-
Carpal bone	A part of the outline of the tubercle of the scaphoid is now seen.
1 <sup>st</sup> metacarpal	Epiphyseal-diaphyseal fusion becomes evident.
Other metacarpals	Epiphyseal-diaphyseal fusion has begun.
Phalanges	Fusion has been partially completed in some epiphyses.

## Female standard

Age: 14 years



Target bones	Major changes
Radius	<ul style="list-style-type: none"><li>• The epiphysis of the radius has capped its shaft.</li><li>• Epiphyseal-diaphyseal fusion has begun.</li></ul>
Ulna	-
Carpal bone	-
1 <sup>st</sup> metacarpal	-
Other metacarpals	Epiphyseal-diaphyseal fusion has been further advanced.
Phalanges	Epiphyseal-diaphyseal fusion has been further advanced.

## Female standard

Age: 15 years



Target bones	Major changes
Radius	-
Ulna	Epiphyseal-diaphyseal fusion has begun.
Carpal bone	-
1 <sup>st</sup> metacarpal	-
Other metacarpals	Epiphyseal-diaphyseal fusion has been advanced.
Phalanges	-

## Female standard

Age: 16 years



Target bones	Major changes
Radius	Epiphyseal-diaphyseal fusion has been further advanced.
Ulna	Epiphyseal-diaphyseal fusion has been further advanced.
Carpal bone	-
1 <sup>st</sup> metacarpal	-
Other metacarpals	-
Phalanges	The epiphyseal lines of the phalanges have been further disappeared.

## Female standard

Age: 17 years



Target bones	Major changes
Radius	The epiphyseal line has been further disappeared.
Ulna	The epiphyseal line has been further disappeared.
Carpal bone	-
1 <sup>st</sup> metacarpal	-
Other metacarpals	-
Phalanges	-

## Female standard

Age: 18 years



Target bones	Major changes
Radius	The epiphyseal line has been nearly disappeared.
Ulna	The epiphyseal line has been nearly disappeared.
Carpal bone	-
1 <sup>st</sup> metacarpal	-
Other metacarpals	-
Phalanges	-